PROCEEDINGS OF SCIENCE

ONLINE ICRC 2021
THE ASTROPARTICLE PHYSICS CONFERENCE
Berlin | Germany
37th International Cosmic Ray Conference
12–23 July 2021

High-energy gamma-ray observations above 10 GeV with CALET on the International Space Station

Masaki Mori[a,*] **on behalf of the CALET Collaboration**
(a complete list of authors can be found at the end of the proceedings)

[a] *Department of Physical Sciences, Ritsumeikan University*
1-1-1 Noji Higashi, Kusatsu, 525-8577, Japan
E-mail: morim@fc.ritsumei.ac.jp

Since the deployment of the CALorimetric Electron Telescope (CALET) on the exposure facility of the Japanese Experiment Module (JEM) 'Kibo' of the International Space Station in 2015, CALET is accumulating cosmic ray data steadily without any serious faults up to now. Although CALET is basically a high-energy cosmic-ray detector, its composite and thick detector structure allow us to separate gamma rays from charged cosmic rays clearly up the TeV energy region. In this paper, analysis of gamma-ray events above 10 GeV obtained by the 'high-energy' triggers, which is the basic trigger mode of CALET for cosmic-ray observations and is always effective regardless of the ISS position in orbit, are reported. Especially, good energy resolution (less than 3% at 10 GeV) of CALET enables us to search for spectral features in the gamma-ray energy spectrum such as lines possibly caused by annihilation of dark matter particles. Gamma-ray events above 10 GeV observed during five years of CALET operation have been analyzed to search for possible line signals in the energy spectra assuming various region-of-interests of the sky depending on the proposed Galactic density profile models. We found no hint of line signals and preliminary upper limits on parameters of the DM annihilation and decay models have been obtained.

37th International Cosmic Ray Conference (ICRC 2021)
July 12th – 23rd, 2021
Online – Berlin, Germany

*Presenter

1. Introduction

The CALorimetric Electron Telescope (CALET) mission [1], which was successfully launched and emplaced on the Japanese Experiment Module (JEM) 'Kibo'-Exposed Facility of the International Space Station (ISS) in 2015 August, has been operational without any serious faults up to the time of this writing (2021 June). The main target of CALET is observation of high-energy cosmic rays, especially electrons, in the energy range from $\sim$ 1 GeV to tens of TeV, but its fine detector structure allows us to observe high-energy gamma-rays from $\sim$ 1 GeV to $\sim$ 10 TeV. Details of our analysis to extract gamma-ray candidates are described in refs. [2, 3].

In this paper, analysis of gamma-ray events above 10 GeV obtained by the 'high-energy' triggers, which is the basic trigger mode of CALET for cosmic-ray observations and is always effective regardless of the ISS position in orbit, are reported. Especially, good energy resolution (less than 3% at 10 GeV) of CALET enables us to search for spectral features in the gamma-ray energy spectrum. Here we report the preliminary results on the search for monochromatic gamma-ray lines possibly caused by annihilation and decay of heavy dark matter particles called weakly interacting massive particles (WIMPs) predicted by a class of various theoretical models [4]. Lower energy gamma-ray observations [5] and transient events [6] are reported separately.

2. CALET detector

The CALorimetric Electron Telescope (CALET) mission [1], which was successfully launched and emplaced on the Japanese Experiment Module-Exposed Facility of the International Space Station (ISS) in 2015 August has been producing scientific data continuously since then.

CALET consists of two scientific instruments. The Calorimeter (CAL) is the main instrument, which is capable of observing high-energy electrons from $\sim$ 1 GeV to $\sim$ 20 TeV, protons, helium, and heavy nuclei from $\sim$ 10 GeV to 1000 TeV and gamma-rays from $\sim$ 1 GeV to $\sim$ 10 TeV. The field of view (FOV) of CAL is $\sim 45^\circ$ from the zenith direction. It consists of three main components: the CHarge Detector (CHD), the IMaging Calorimeter (IMC), and the Total AbSorption Calorimeter (TASC). Details of the detector is described elsewhere [7]. Here we just mention that we have two trigger modes of the CALET/CAL (calorimeter, the main instrument of CALET) related to gamma-ray observation: a high-energy (HE) mode with an energy threshold $\sim$ 10 GeV used in normal operation irrespective of geomagnetic latitude, and a low-energy gamma-ray (LE-γ) mode with a threshold $\sim$ 1 GeV, activated when the geomagnetic latitude is below 20° and following a CALET Gamma-ray Burst Monitor (CGBM) burst trigger (see ref. [8] for details on our trigger scheme).

The CAL gamma-ray performance and initial CAL gamma-ray results for steady sources are described in ref. [2]. The energy resolution and the angular resolution for gamma rays are estimated as 3% and 0.4°, respectively, at 10 GeV [2, 7], and the energy dependence of its energy resolution is plotted in Fig. 1 (left), which shows its good performance in the high-energy region thanks to the thick calorimetric configuration of CAL. The effective area in the HE mode is shown in Fig. 1 (right) which has a peak of about 400 cm^2 at 30 GeV for vertical incidence.

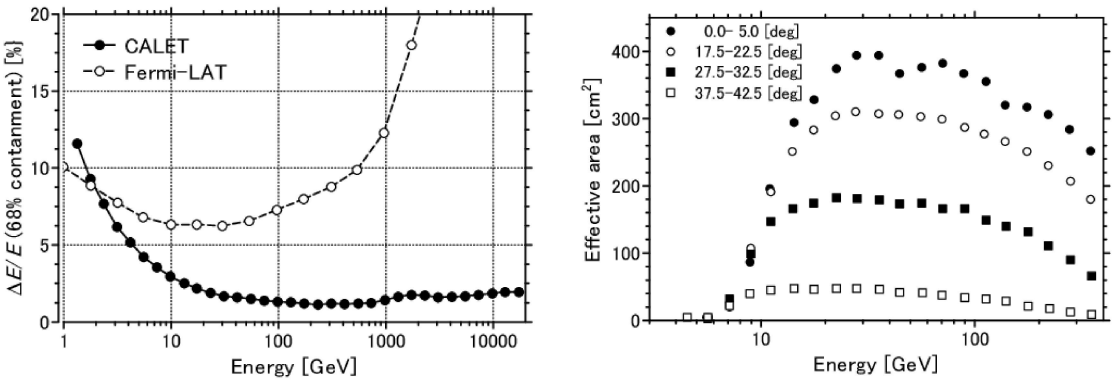

Figure 1: (*Left*) Energy resolution of CALET for electromagnetic showers as a function of energy [7]. Also plotted is the energy resolution of Fermi-LAT (P8R3SOURCE_V2, Total [9]). (*Right*) Effective area of CALET for gamma rays in the high-energy mode as a function of energy for various angles of incidence.

3. Gamma-ray line signal from dark matter

If the Weakly Interacting Massive Particles (WIMPs), popular candidates for the dark matter (DM) in the Universe, annihilate or decay into a photon and a neutral particle (such as another photon or Z^0 boson), approximately monoenergetic gamma rays will be produced in the rest frame. For nonrelativistic DM particles such as those constituting the Galactic halo, this may give rise to a monoenergetic ("line") photon signal in the smooth spectrum, which most likely follows power-law form, of the standard astrophysical emission [4].

If the spectral line is produced by DM annihilation into a pair of gamma rays, the expected gamma-ray flux is given by

$$\left(\frac{\mathrm{d}\Phi}{\mathrm{d}E}\right)_{\mathrm{ann}} = \frac{\langle\sigma v\rangle_{\gamma\gamma}}{8\pi m_{\mathrm{DM}}^2}\left(\frac{\mathrm{d}N}{\mathrm{d}E}\right)_{\mathrm{ann}}\left[\int_{\mathrm{ROI}}\mathrm{d}\Omega\int_{\mathrm{l.o.s.}}\mathrm{d}s\,\rho(r)^2\right] \tag{1}$$

where $\langle\sigma v\rangle_{\gamma\gamma}$ is the averaged DM annihilation cross section times relative velocity for two-photon production, m_{DM} is the mass of the DM particle, $(\mathrm{d}N/\mathrm{d}E)_{\mathrm{ann}} = 2\delta(E_\gamma - E)$, and $E_\gamma = m_{\mathrm{DM}}$. For lines generated by DM decay into a gamma ray and a second neutral particle, the expected flux is given by

$$\left(\frac{\mathrm{d}\Phi}{\mathrm{d}E}\right)_{\mathrm{dec}} = \frac{1}{4\pi\tau_{\mathrm{DM}}m_{\mathrm{DM}}^2}\left(\frac{\mathrm{d}N}{\mathrm{d}E}\right)_{\mathrm{dec}}\left[\int_{\mathrm{ROI}}\mathrm{d}\Omega\int_{\mathrm{l.o.s.}}\mathrm{d}s\,\rho(r)\right] \tag{2}$$

where τ_{DM} is the lifetime of the DM particle, $(\mathrm{d}N/\mathrm{d}E)_{\mathrm{dec}} = \delta(E_\gamma - E)$, and $E_\gamma = m_{\mathrm{DM}}/2$. The quantities in the square brackets in above two equations are so-called J factors ($J_{\mathrm{ann}}/J_{\mathrm{dec}}$) and are proportional to the expected intensity of gamma-ray emission from DM annihilation or decay in a given region-of-interest (ROI) assuming a specific DM density distribution $\rho(r)$ of the Galactic halo, where r is the radial distance from the Galactic center. The last integrals are performed along line-of-sight (l.o.s.) from us toward a specific direction.

4. Analysis

We analyzed the CALET gamma-ray candidates to search for a line gamma-ray signal using the data during about five year of observation, from October 13, 2015 to September 30, 2020, and

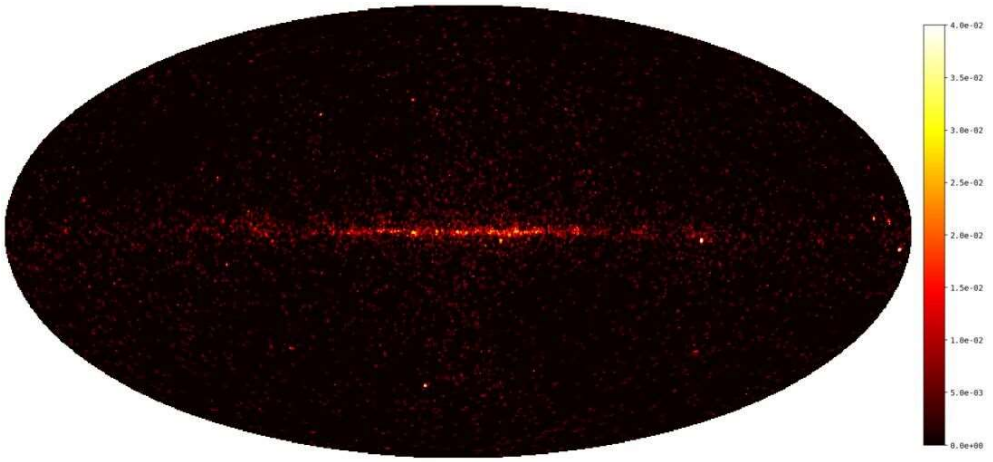

Figure 2: Skymap of gamma-ray events (HE trigger, > 10 GeV) shown in the Galactic coordinates.

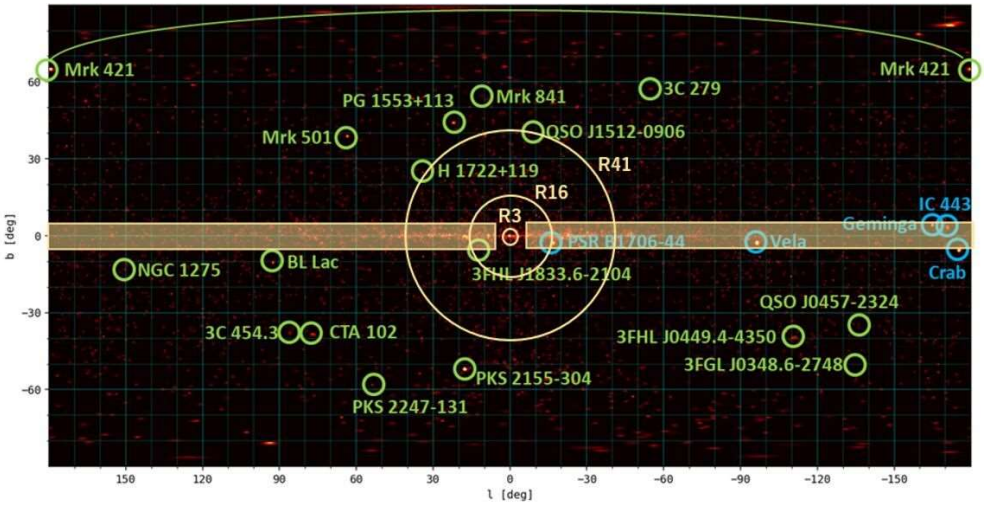

Figure 3: Regions of interest (ROI) in the skymap used for gamma-ray line signals. See text for details.

obtained 12,260 gamma-ray candidates in the HE trigger mode. The skymap of these events are shown in Fig. 2 without correction of non-uniform exposure (about 90% (50%) of the whole sky is covered with more than 60% (80%) of the maximum exposure).

We used five regions of interest in the skymap for gamma-ray line search. They are defined as circular regions of radius $R_{\rm GC}$ centered on the Galactic center with $|b| < 5^\circ$ and $|\ell| > 6^\circ$ masked, following to ref. [10], as shown in Fig. 3. They are based on four smooth parametrizations for the distribution of DM in the Galaxy ('NFW contracted', 'NFW', 'Einasto' and 'Isothemal': see ref. [10] for definitions). Four regions, called as R3 ($R_{\rm GC} = 3^\circ$, optimized for the contracted NFW profile), R16 ($R_{\rm GC} = 16^\circ$, optimized for the Einasto profile), R41 ($R_{\rm GC} = 41^\circ$, optimized for the NFW profile) and R90 ($R_{\rm GC} = 90^\circ$, optimized for the isothermal profile), are used for annihilating DM models, and another region, called as R180 ($R_{\rm GC} = 180^\circ$) for decayng DM models. We mask bright point sources shown in Fig. 3 as 1°-radius circles each.

We selected gamma-ray candidates in each ROI from our samples, and calculated energy

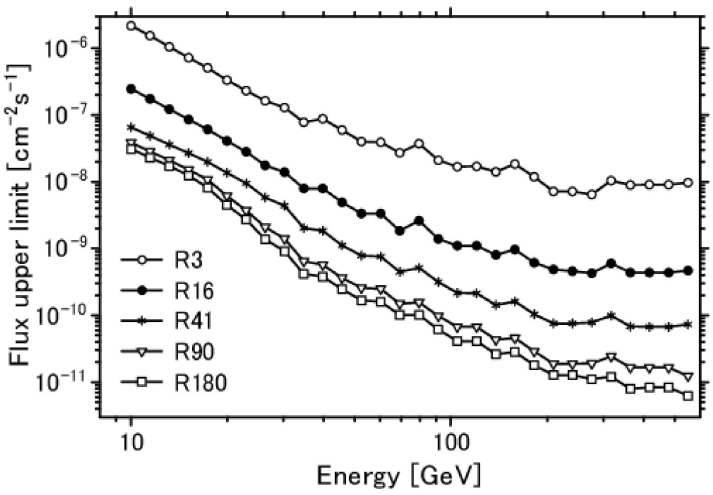

Figure 4: Upper limits (95% C.L.) on gamma-ray line signal for each ROI from the CALET observation. See text for definitions of ROI.

Galactic halo profile	Annihilation ROI	Annihilation $J_{\rm ann}$ [GeV^{2}cm^{-6} kpc]	Decay ROI	Decay $J_{\rm dec}$ [GeV cm^{-3} kpc]
NFW contracted	R3	37.3	R180	77.6
Einasto	R16	30.0	R180	79.0
NFW	R41	29.1	R180	78.0
Isothermal	R90	22.4	R180	76.7

Table 1: J factors calculated for each ROI after applying point-source cuts. See text for Galactic halo profiles and definitions of ROI.

spectra (10 bins per decade) by summing up exposures computed as HealPix equi-solid-angle bins of resolution index 6 (49,152 bins) [12]. Then, 95% C.L. upper limits on line signals have been calculated by adding the assumed line signals to the observed spectra which raise the reduced χ^2 (where only statistical errors are taken into account) for the power-law fit by 3.94 [13]. (When there is no entry in the energy bin, we assigned 1.29 events as the 95% C.L. limit following ref.[14].) Here the assumed line signal has been broadened by a Gaussian distribution with the energy resolution of CALET, shown in Fig. 1 (left), before adding to the spectra. We assumed the monochromatic energy of gamma rays to be $10^{1+0.06i}$ GeV ($i = 0, \cdots, 29$) for this calculation so that there should be no interference effect with energy bin boundaries. The resulting upper limits on fluxes are plotted in Fig. 4 as a function of the assumed line energy.

The upper limits on DM annihilation and decay parameters have been calculated based on equations (1) and (2) following [10]: The J factors ($J_{\rm ann}/J_{\rm dec}$) have been calculated for each ROI optimized for the assumed four models describing the Galactic halo density profiles, and tabulated in Table 1. Then upper limits on $\langle\sigma v\rangle$ and τ_{DM} have been calculated with the flux upper limits given in Fig. 4, and preliminary results are plotted for each density profile in Fig. 5 for annihilation and Fig. 6 for decay, respectively, in comparison with the limits reported in ref. [11]. Fig. 6 shows the case of the NFW profile only, but limits for τ_{DM} are almost model-independent (see Table 1).

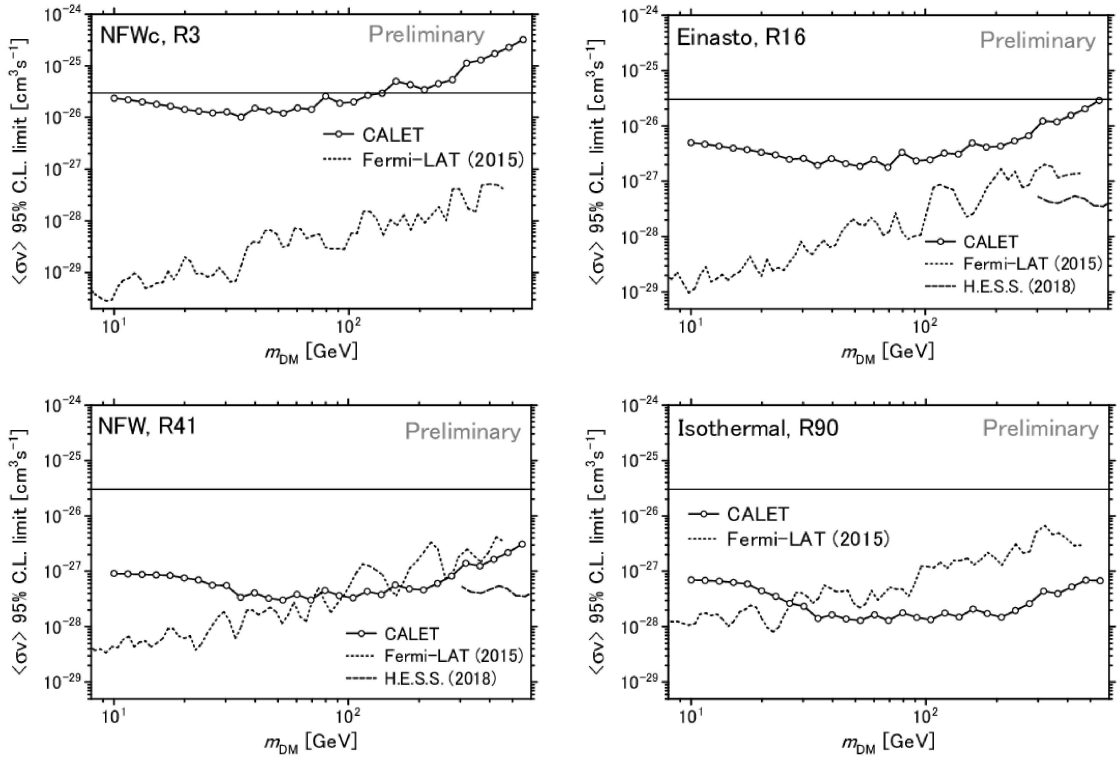

Figure 5: Upper limits on DM velocity-averaged annihilation cross section as a function of the DM mass for each ROI. Also shown are those given by Fermi-LAT [11] and H.E.S.S. [15] for comparison. Horizontal thin lines show the canonical thermal relic cross section of 3×10^{-26} cm^3 s^{-1}.

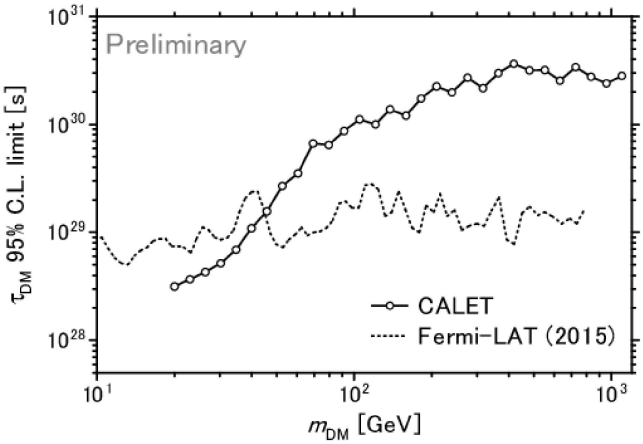

Figure 6: Upper limits on DM decay lifetime assuming the NFW halo profile. ROI in this case is R180. Limits assuming other profiles are almost indistinguishable. Also shown are those given by Fermi-LAT [11] for comparison.

5. Summary

Gamma-ray events above 10 GeV observed during five years of operation of the CALET detector onboard the International Space Station have been analyzed to search for possible line signals in the energy spectra assuming various region-of-interests of the sky depending on the proposed Galactic halo density profile models. We found no hint of line signals and gave upper limits on parameters of the DM annihilation and decay models, although these limits, taking account of only statistical errors, are still preliminary. We are now studying possible systematic errors in our limits.

Our velocity-averaged cross section limits lie in the range $\langle\sigma v\rangle_{\gamma\gamma} \sim 10^{-28}$–$10^{-25}$ cm^3 s^{-1}, with the precise limit depending on the DM mass and the DM density profile assumed for the Galaxy; gentler profiles which produce wider distribution around the Galactic center are constrained more strongly, mainly because we have more events for larger ROI and statistical errors are reduced. The limits are a factor up to 30 times below the canonical thermal relic cross section of $\langle\sigma v\rangle_{\rm WIMP} \sim 3 \times 10^{-26}$ cm^3 s^{-1} [4] and therefore constrain models in which DM particles can annihilate to standard model particles through tree-level diagrams. However, since DM is constrained to be electrically neutral to a very good approximation, WIMP interactions in most models produce monochromatic gamma rays only through higher-order processes, the cross sections of which are typically suppressed by 3 or more orders of magnitude [4]. This means that our limits do not disfavor the WIMP hypothesis in general. Comparing with the Fermi-LAT results [11], our limits on the velocity-averaged cross section are extended towards a slightly heavier DM masses and are comparable for gentler Galactic halo density profiles (NFW and isothermal), but are worse for cuspier ones (NFWc and Einasto). Our limits on the DM decay lifetime are also extended towards a slightly heavier DM masses and could be better than Fermi-LAT results [11] for $m_{\rm DM} \gtrsim 50$ GeV, although we have not taken systematical errors into account yet.

Acknowledgment This work was supported by JSPS KAKENHI Grant Numbers JP16K05382 and JP19H05608.

References

[1] S. Torii for the CALET Collaboration, "The CALorimetric Electron Telescope (CALET) on the ISS: Preliminary Results from On-orbit Observations since October, 2015", *Proc. 35th ICRC* (Busan, Korea, 2017), PoS (ICRC2017) 1092; Y. Asaoka for the CALET Collaboration, "The CALorimetric Electron Telescope (CALET) on the International Space Station", *Proc. 36th ICRC* (Madison, USA, 2019), PoS (ICRC2019) 001; Pier S, Marocchesi for the CALET collaboration, "New Results from the first 5 years of CALET observations on the International Space Station", in this conference (ID: 786).

[2] N. Cannady for the CALET Collaboration, "High-Energy Gamma-ray Observations Using the CALorimetric Electron Telescope", *Proc. 35th ICRC* (Busan, Korea, 2017), PoS (ICRC2017) 720.

[3] N. Cannady et al., "Characteristics and Performance of the CALorimetric Electron Telescope (CALET) Calorimeter for Gamma-Ray Observations", *Astrophys. J. Suppl.* **238**, 5 (2018).

[4] For a review, see, for example, J.L. Feng, "Dark matter candidates from particle physics and methods of detection", *Ann. Rev. Astron. Astrophys.* **48**, 495 (2010).

[5] N. Cannady for the CALET Collaboration, "Low-energy gamma-ray observations above 1 GeV with CALET on the International Space Station", in this conference (ID: 322).

[6] Y. Kawakubo for the CALET Collaboration, "Gamma-ray burst observation & gravitational wave event follow-up with CALET on the International Space Station", in this conference (ID: 817).

[7] Y. Asaoka et al., "Energy calibration of CALET onboard the International Space Station", *Astropart. Phys.* 91, 1 (2017).

[8] Y. Asaoka et al., "On-orbit operations and offline data processing of CALET onboard the ISS", *Astropart. Phys.* **100**, 29 (2018).

[9] "Fermi LAT Performance", https://www.slac.stanford.edu/exp/glast/groups/canda/lat_Performance.htm

[10] M. Ackermann et al., "Search for gamma-ray spectral lines with the Fermi Large Area Telescope and dark matter implications", *Phys. Rev. D* **88**, 082002 (2013)

[11] M. Ackermann et al., "Updated Search for spectral lines from Galactic dark matter interactions with pass 8 data from the Fermi Large Area Telescope", *Phys. Rev. D* **91**, 122002 (2015)

[12] K.M. Górski et al., "HEALPIX – a Framework for High Resolution Discretization, and Fast Analysis of Data Distributed on the Sphere", *Astrophys. J.* **622**, 759 (2005).

[13] F. James, "Interpretation of the shape of the likelihood function around its minimum", *Comp. Phys. Com.* **20**, 29 (1980).

[14] G. J. Feldmann and R. D. Cousins, "A Unified Approach to the Classical Statistical Analysis of Small Signals", *Phys. Rev. D* **57**, 3873 (1998).

[15] H. Abdallah et al., "Search for γ-Ray Line Signals from Dark Matter Annihilations in the Inner Galactic Halo from 10 Years of Observations with H.E.S.S.", *Phys. Rev. Lett.* **120**, 201101 (2018).

Full Authors List: CALET Collaboration

O. Adriani[1,2], Y. Akaike[3,4], K. Asano[5], Y. Asaoka[5], E. Berti[1,2], G. Bigongiari[6,7], W. R. Binns[8], M. Bongi[1,2], P. Brogi[6,7], A. Bruno[9,10], J. H. Buckley[8], N. Cannady[11,12,13], G. Castellini[14], C. Checchia[6], M. L. Cherry[15], G. Collazuol[16,17], K. Ebisawa[18], A. W. Ficklin[15], H. Fuke[18], S. Gonzi[1,2], T. G. Guzik[15], T. Hams[11], K. Hibino[19], M. Ichimura[20], K. Ioka[21], W. Ishizaki[5], M. H. Israel[8], K. Kasahara[22], J. Kataoka[23], R. Kataoka[24], Y. Katayose[25], C. Kato[26], N. Kawanaka[27,28], Y. Kawakubo[15], K. Kobayashi[3,4], K. Kohri[29], H. S. Krawczynski[8], J. F. Krizmanic[11,12,13], J. Link[11,12,13], P. Maestro[6,7], P. S. Marrocchesi[6,7], A. M. Messineo[30,7], J.W. Mitchell[12], S. Miyake[32], A. A. Moiseev[33,12,13], M. Mori[34], N. Mori[2], H. M. Motz[35], K. Munakata[26], S. Nakahira[18], J. Nishimura[18], G. A. de Nolfo[9], S. Okuno[19], J. F. Ormes[36], N. Ospina[16,17], S. Ozawa[37], L. Pacini[1,14,2], P. Papini[2], B. F. Rauch[8], S. B. Ricciarini[14,2], K. Sakai[11,12,13], T. Sakamoto[38], M. Sasaki[33,12,13], Y. Shimizu[19], A. Shiomi[39], P. Spillantini[1], F. Stolzi[6,7], S. Sugita[38], A. Sulaj[6,7], M. Takita[5], T. Tamura[19], T. Terasawa[40], S. Torii[3], Y. Tsunesada[41], Y. Uchihori[42], E. Vannuccini[2], J. P. Wefel[15], K. Yamaoka[43], S. Yanagita[44], A. Yoshida[38], K. Yoshida[22], and W. V. Zober[8]

[1]Department of Physics, University of Florence, Via Sansone, 1, 50019 Sesto, Fiorentino, Italy, [2]INFN Sezione di Florence, Via Sansone, 1, 50019 Sesto, Fiorentino, Italy, [3]Waseda Research Institute for Science and Engineering, Waseda University, 17 Kikuicho, Shinjuku, Tokyo 162-0044, Japan, [4]JEM Utilization Center, Human Spaceflight Technology Directorate, Japan Aerospace Exploration Agency, 2-1-1 Sengen, Tsukuba, Ibaraki 305-8505, Japan, [5]Institute for Cosmic Ray Research, The University of Tokyo, 5-1-5 Kashiwa-no-Ha, Kashiwa, Chiba 277-8582, Japan, [6]Department of Physical Sciences, Earth and Environment, University of Siena, via Roma 56, 53100 Siena, Italy, [7]INFN Sezione di Pisa, Polo Fibonacci, Largo B. Pontecorvo, 3, 56127 Pisa, Italy, [8]Department of Physics and McDonnell Center for the Space Sciences, Washington University, One Brookings Drive, St. Louis, Missouri 63130-4899, USA, [9]Heliospheric Physics Laboratory, NASA/GSFC, Greenbelt, Maryland 20771, USA, [10]Department of Physics, Catholic University of America, Washington, DC 20064, USA, [11]Center for Space Sciences and Technology, University of Maryland, Baltimore County, 1000 Hilltop Circle, Baltimore, Maryland 21250, USA, [12]Astroparticle Physics Laboratory, NASA/GSFC, Greenbelt, Maryland 20771, USA, [13]Center for Research and Exploration in Space Sciences and Technology, NASA/GSFC, Greenbelt, Maryland 20771, USA, [14]Institute of Applied Physics (IFAC), National Research Council (CNR), Via Madonna del Piano, 10, 50019 Sesto, Fiorentino, Italy, [15]Department of Physics and Astronomy, Louisiana State University, 202 Nicholson Hall, Baton Rouge, Louisiana 70803, USA, [16]Department of Physics and Astronomy, University of Padova, Via Marzolo, 8, 35131 Padova, Italy, [17]INFN Sezione di Padova, Via Marzolo, 8, 35131 Padova, Italy, [18]Institute of Space and Astronautical Science, Japan Aerospace Exploration Agency, 3-1-1 Yoshinodai, Chuo, Sagamihara, Kanagawa 252-5210, Japan, [19]Kanagawa University, 3-27-1 Rokkakubashi, Kanagawa, Yokohama, Kanagawa 221-8686, Japan, [20]Faculty of Science and Technology, Graduate School of Science and Technology,, Hirosaki University, 3, Bunkyo, Hirosaki, Aomori 036-8561, Japan, [21]Yukawa Institute for Theoretical Physics, Kyoto University, Kitashirakawa Oiwakecho, Sakyo, Kyoto 606-8502, Japan, [22]Department of Electronic Information Systems, Shibaura Institute of Technology, 307 Fukasaku, Minuma, Saitama 337-8570, Japan, [23]School of Advanced Science and Engineering, Waseda University, 3-4-1 Okubo, Shinjuku, Tokyo 169-8555, Japan, [24]National Institute of Polar Research, 10-3, Midori-cho, Tachikawa, Tokyo 190-8518, Japan, [25]Faculty of Engineering, Division of Intelligent Systems Engineering, Yokohama National University, 79-5 Tokiwadai, Hodogaya, Yokohama 240-8501, Japan, [26]Faculty of Science, Shinshu University, 3-1-1 Asahi, Matsumoto, Nagano 390-8621, Japan, [27]Hakubi Center, Kyoto University, Yoshida Honmachi, Sakyo-ku, Kyoto 606-8501, Japan, [28]Department of Astronomy, Graduate School of Science, Kyoto University, Kitashirakawa Oiwake-cho, Sakyo-ku, Kyoto 606-8502, Japan, [29]Institute of Particle and Nuclear Studies, High Energy Accelerator Research Organization, 1-1 Oho, Tsukuba, Ibaraki 305-0801, Japan, [30]University of Pisa, Polo Fibonacci, Largo B. Pontecorvo, 3, 56127 Pisa, Italy, [31]Astroparticle Physics Laboratory, NASA/GSFC, Greenbelt, Maryland 20771, USA, [32]Department of Electrical and Electronic Systems Engineering, National Institute of Technology, Ibaraki College, 866 Nakane, Hitachinaka, Ibaraki 312-8508, Japan [33]Department of Astronomy, University of Maryland, College Park, Maryland 20742, USA, [34]Department of Physical Sciences, College of Science and Engineering, Ritsumeikan University, Shiga 525-8577, Japan, [35]Faculty of Science and Engineering, Global Center for Science and Engineering, Waseda University, 3-4-1 Okubo, Shinjuku, Tokyo 169-8555, Japan, [36]Department of Physics and Astronomy, University of Denver, Physics Building, Room 211, 2112 East Wesley Avenue, Denver, Colorado 80208-6900, USA, [37]Quantum ICT Advanced Development Center, National Institute of Information and Communications Technology, 4-2-1 Nukui-Kitamachi, Koganei, Tokyo 184-8795, Japan, [38]College of Science and Engineering, Department of Physics and Mathematics, Aoyama Gakuin University, 5-10-1 Fuchinobe, Chuo, Sagamihara, Kanagawa 252-5258, Japan, [39]College of Industrial Technology, Nihon University, 1-2-1 Izumi, Narashino, Chiba 275-8575, Japan [40]RIKEN, 2-1 Hirosawa, Wako, Saitama 351-0198, Japan, [41]Division of Mathematics and Physics, Graduate School of Science, Osaka City University, 3-3-138 Sugimoto, Sumiyoshi, Osaka 558-8585, Japan, [42]National Institutes for Quantum and Radiation Science and Technology, 4-9-1 Anagawa, Inage, Chiba 263-8555, Japan, [43]Nagoya University, Furo, Chikusa, Nagoya 464-8601, Japan, [44]College of Science, Ibaraki University, 2-1-1 Bunkyo, Mito, Ibaraki 310-8512, Japan